ARCHIVES of FOUNDRY ENGINEERING

DOI: 10.2478/v10266-012-0018-9

Published quarterly as the organ of the Foundry Commission of the Polish Academy of Sciences

VERSITA

ISSN (1897-3310)
Volume 12
Issue 1/2012

93 – 98

# Evaluation of Porosity in Al Alloy Die Castings

**M. Říhová [a]*, J.Cech [a], J. Havlíčková [b]**

[a] Institute of Manufacturing Technology, Department of Foundry Engineering,
Faculty of Mechanical Engineering, Brno University of Technology, Technická 2896/2, Brno, Czech Republic
[b] TOS KURIM - OS, a.s., Štefánikova 41/110, Brno ,Czech
*Corresponding author. E-mail address: marketarihova@seznam.cz

Received 01.02.2012; accepted in revised form 28.03.2012

## Abstract

Mechanical properties of an Al-alloy die casting depend significantly on its structural properties. Porosity in Al-alloy castings is one of the most frequent causes of waste castings. Gas pores are responsible for impaired mechanical-technological properties of cast materials. On the basis of a complex evaluation of experiments conducted on AlSi9Cu3 alloy samples taken from the upper engine block which was die-cast with and without local squeeze casting it can be said that castings manufactured without squeeze casting exhibit maximum porosity in the longitudinal section. The area without local squeeze casting exhibits a certain reduction in mechanical properties and porosity increased to as much as 5%. However, this still meets the norms set by SKODA AUTO a.s.

**Keywords:** AlSi9Cu3 alloy casting of upper engine block, Porosity, Mechanical values, Simulation

## 1. Introduction

To design engine blocks (e.g. for SKODA Fabia) it is necessary to know exactly the strength, structure, and stress conditions in the whole cross-section of the casting. In the case of geometrically complex castings (such as engine block castings) the different conditions of melt cooling and solidification result in that the mechanical, structural and stress relations are changed locally. It cannot be assumed that the properties are constant over the entire cross-section of the casting wall.

Mechanical properties of a gravity casting ($R_m$, $R_{p0.2}$, A, HB, etc.) depend to a high degree on its structural properties (grain size, secondary arm spacing of dendrites (DAS in the following), eutectic phase, porosity, etc.). These properties also depend on the chemical composition and metallurgical treatment of the melt (grain refinement, alloying), parameters of casting and solidification processes, and additional treatment (heat treatment). In Al-Si alloys the structure is given by the primary dendrite growth of the Al-enriched α-phase and by interdendritic eutectics. DAS and the type of the formation and distribution of hard eutectic Si particles or intermetallic phases are substantial structural features that influence the strength properties after melt solidification.

The most important criterion in the description of dendrite structure is the spacing of secondary dendrite axes, referred to as dendrite arm spacing (DAS). The main idea, supported by a number of experiments, consists in claiming that the smaller the DAS, the better the mechanical properties of an alloy [1].
The value of DAS does not depend on the size of primary grains, state of crystallization nuclei or the effect of inoculation but, above all, on the cooling rate in the solidification interval.

$$DAS = a \quad t_{tuh}^{\frac{1}{3}} \qquad [\mu m] \tag{1}$$

a – material constant [µm/ $s^{-\frac{1}{3}}$ ]

t – solidification time [s]

The relations between the mechanical properties and the structure given by the constants in the Hall-Petch relation are rendered by the equations

$$R_{p0,2} = K_1 + \frac{K_2}{\sqrt{DAS}} \qquad [MPa] \tag{2}$$

$$R_m = K_3 + \frac{K_4}{\sqrt{DAS}} \qquad [MPa] \tag{2a}$$

where $K_2$, $K_4$ are material constants [MPa.µm $^{\frac{1}{2}}$ ]

The size of primary grains α (Al) in casting alloys is usually in the range from 1 to 10 mm.

DAS in castings ranges from 10 to 150 µm. The larger the spacing, the greater the probability of the occurrence of porosity and shrinkages. The goal is therefore to have this spacing as small as possible.

The magnitude of DAS is connected with a number of other structural phenomena. The finer the structure (i.e. lower DAS value), the smaller the segregation distances. Thus when the extent of segregations is smaller, there appear smaller particles of intermetallic inclusions. Impurities are separated as separate particles in interdendritic spaces, the chemical composition of the alloy is more homogeneous, and micro porosity is distributed more favourably.

To obtain a fast quantitative determination of the geometric parameters of the structure (inclusions, hollow spaces) the shape factor *f* or its reciprocal value, the sphericity factor *s* is used.

$$f = \frac{4\pi A_p}{U^2} \leq 1 \qquad [-] \tag{3}$$

$$s = \frac{1}{f} = \frac{U^2}{4\pi A_p} \geq 1 \qquad [-] \tag{4}$$

where $A_p$ is the blow-hole circumference [µm]

U is the perimeter of cross-section area of structure element [µm$^2$]

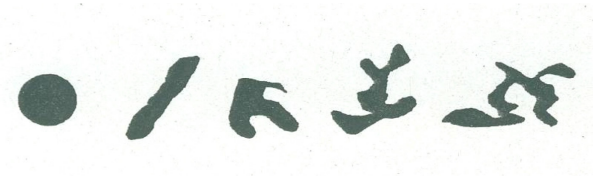

s=1 s=2 s=3 s=4 s=5

Fig. 1. Shape of pores with different sphericity factors "s"

For a circular section the value of sphericity factor is 1 while for more complex shapes it is >1 (Fig. 1). It responds sensitively to changes in the geometry of inclusions and internal cavities, which are connected with changes in mechanical properties. Pores with the sphericity factor s>1 exhibit, under identical porosity P, a higher measure of matrix interruption than spherical pores with s=1, which corresponds to a porosity that is higher by factor s.

With increasing factor s the notch effect of pores increases, the appearance of cracks in the structure increases and this shows up in the strength of the material. To determine the mechanical properties $R_m$ and $R_{p0.2}$ the following relations are used [2]:

$$R_m = R_m^{\,o}(1 - s\,P) \qquad [MPa] \tag{5}$$

$$R_{p0,2} = R_{p0,2}^{\,o}(1 - P) \qquad [MPa] \tag{6}$$

where $R_m$, $R_{p0.2}$ are the ultimate strength and yield point of porous material [MPa]

$R_m$, $R_{p0.2}$ are the ultimate strength and yield point of material without pores [MPa]

The porosity of die-castings is usually due to the appearance of a combination of micro shrinkages and blow-holes. When the mechanism of blow-hole formation predominates, the pores are rather of the spherical shape; if the micro shrinkage mechanism predominates, the cavities are of ragged shape and copy the dendritic structure of the metal.

$$P = \frac{S_p}{S_0} \cdot 100 \qquad [\%] \tag{7}$$

$S_p$ is the pore area [mm$^2$]
$S_0$ is the total selected area of metal [mm$^2$]
P is the porosity [%]

## 2. Experimental part

The subject of experiment was a spark-ignition engine, cylinder block of type designation EA11103D (Fig. 2)

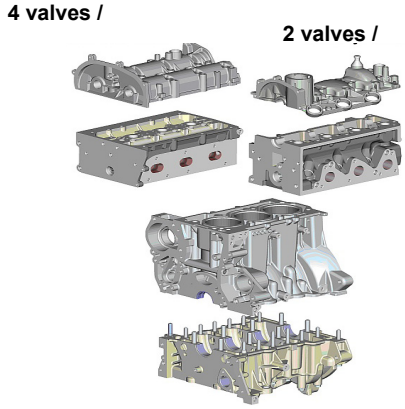

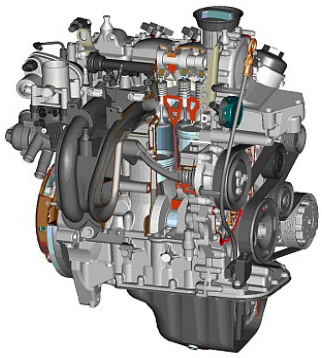

Fig. 2. EA 111 03D three-cylinder spark-ignition engine made of AlSi9Cu3 (Fe) alloy [3]

Chosen for evaluation was the upper part casting R 03D 103 019M made of AlSi9Cu3 alloy, with and without local squeeze casting (LSC). Casting parameters for the upper part of the cylinder block are given in Table 1.

Table 1.
Casting parameters for upper part R 03 D 103 M and lower part R 03D 103 166 H [3]

| Type of casting | **R 03D 103 019 M with LSC** | **R 03D 103 019 M without LSC** |
|---|---|---|
| Casting machine | IDRA 37 | IDRA 35 |
| Parameter/date | 26.8.2008 | 25.8.2008 |
| Holding temperature | 665 °C | 660 °C |
| 1st speed [m/s] | 0,15 | 0,14 |
| 2nd speed [m/s] | 6,14 | 5,6 |
| Squeeze [bar] | 323 | 353 |
| Pressure LSC [bar] | 500-600 | --- |
| Solidification [sec] | 32 | 32 |
| 1st trace [mm] | 180 | 180 |
| 2nd trace [mm] | 320 | 520 |
| 3rd trace [mm] | 330 | 530 |
| VAK start [mm] | 200 | 200 |
| VAK stop [mm] | 290 | 490 |
| Cycle [sec] | 167 | 167 |

In the new, adapted engine block the geometry of outer dimensions has been preserved; due to a change in manufacturing technology the bearing area of crankshaft support is different (Fig. 3).

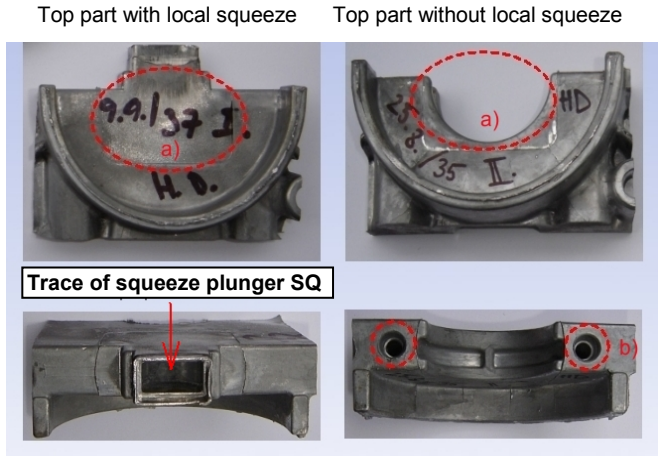


Fig. 3. Different shapes of the bearing area of upper part of old block (with LSC) and new block [3]

In the case of die castings without local squeeze it can be expected (as evidenced by computer simulation) that the greatest porosity increase is exactly in the bearing area. For this reason the test samples were taken from the bearing area (4th bearing) of the upper part of the engine block (Fig. 4).

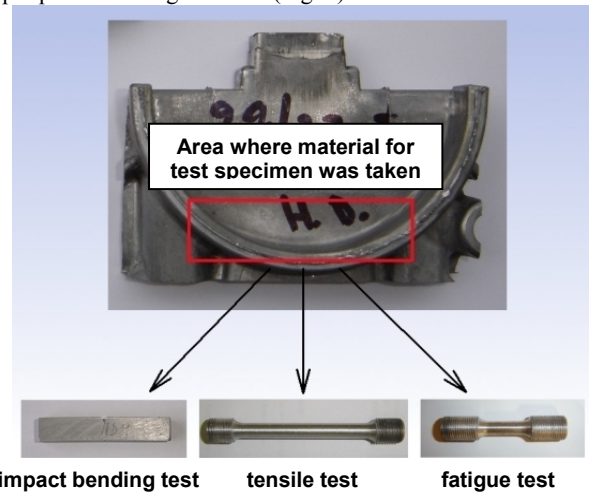


Fig. 4. 4-th bearing area cut out of top part [4]

For better orientation, the following marking was introduced: HDS – upper part, die-cast with local squeeze casting, the current block; HD – upper part, die-cast without local squeeze casting, the new part. Tensile test rods were prepared, according to the DIN standard, from the prisms cut. Tensile characteristics were measured in BUT FME IMT on a TIRA-Test 2300 device [4]. Samples for longitudinal and transverse sections were taken from tensile test rods (Fig. 5).

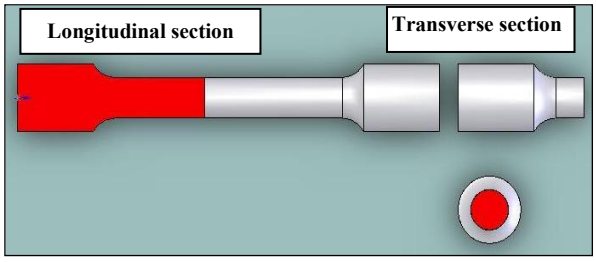

Fig. 5. Approximate sites of longitudinal and cross sections of rods [5]

The data sets underwent statistical tests, in which potential gross mistakes were removed. Statistical evaluation was performed using the Mathcad 13 software.

## 2.1. Evaluation of porosity (P)

Ruptured rods from the tensile test were used for the preparation of metallographic polished samples. After polishing, the porosity of several original samples was tested using the AnalySIS (Olympus) program[4-9]. In another group of samples the Stream Motion (Olympus) program was used to evaluate porosity. This program gives a more detailed picture of the magnified area of the sample and also enables setting a filter for discarding smaller objects. For the measurement of longitudinal and transverse section samples five rectangular areas were chosen such that they represented the whole section area (Fig. 6).

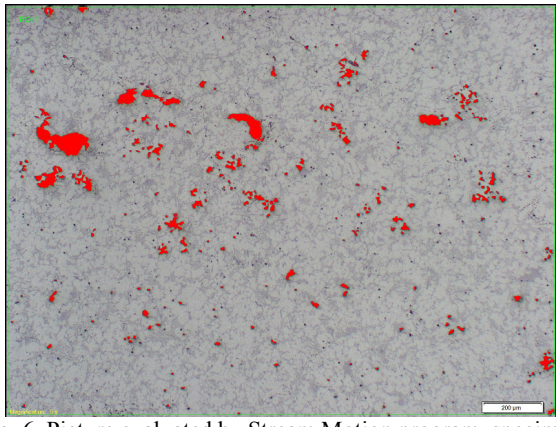
Fig. 6. Picture evaluated by Stream Motion program, specimen HD7, measurement No 7 [6]

Evaluation was performed for 44 longitudinal and 53 transverse sections of HD samples, and for 38 longitudinal and 46 transverse sections of HDS samples.

## 2.2. Processing of experimental measurements

From earlier works [4-9] a total of 84 measurements for HDS samples and 97 HD samples were processed. Table 2 gives all the porosity values established using the image analysis method. The graphic version can be seen in Fig. 7.

Table 2.
Comprehensive overview of average porosity for all measurements of upper engine block [6]

| Sample marking | Sample part | Porosity P [%] | Sample marking | Sample part | Porosity P [%] |
|---|---|---|---|---|---|
| HDS 1 | longitudinal | 0,55 | HD 6 | longitudinal | 1,61 |
| | transverse | 1,05 | | transverse | 3,31 |
| HDS 3 | longitudinal | 0,72 | HD 7 | longitudinal | 1,51 |
| | transverse | 0,77 | | transverse | 1,86 |
| HDS 6 | longitudinal | 0,42 | HD 8 | longitudinal | 1,18 |
| | transverse | 0,91 | | transverse | 1,29 |
| HDS 10 | longitudinal | 0,48 | HD 10 | longitudinal | 1,47 |
| | transverse | 1,47 | | transverse | 2,16 |
| HDS 11 | longitudinal | 0,52 | HD 11 | longitudinal | 0,90 |
| | transverse | 0,66 | | transverse | 2,63 |
| HDS 12 | longitudinal | 0,62 | HD 12 | longitudinal | 1,24 |
| | transverse | 0,69 | | transverse | 2,29 |
| - | - | | HD 13 | longitudinal | 0,68 |
| | | | | transverse | 1,54 |
| **Average porosity P [%]** | longitudinal | 0,55 | **Average porosity P [%]** | longitudinal | 1,23 |
| | transverse | 0,92 | | transverse | 2,15 |
| **Total average P [%]** | 0,74 | | **Total average** P [%] | 1,69 | |

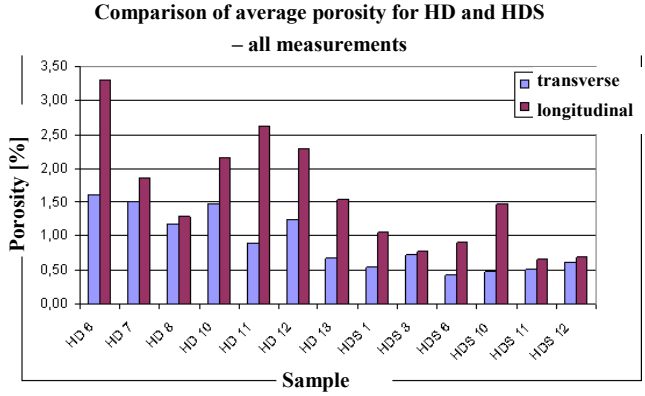

Fig. 7. Graphic expression of all porosity measurements for upper part [6]

In the case of die-casting the upper part, the sets of values measured exhibit, with increasing porosity, both decreasing and increasing curves for $R_m$ and $R_{p0.2}$. Porosity evaluation is greatly affected by the exact site of sample selection on the casting and by local structure and stress conditions because the properties are not of a constant nature across the whole cross-section of the casting wall. A greater occurrence of porosity appears in castings without local squeeze. The overall average for HD samples is ca. 1% higher than in HDS samples. The greatest occurrence of areas with absent metal was established for longitudinal bearing sections of HD samples (over 2% on average).[9-10]

The lowest average porosity for all these samples was found in the transverse section of the casting with local squeeze casting (0.55%). Major differences could be established for sections through the HD sample – the transverse section lacked 1.23% on average and the longitudinal section as much as 2.15% of alloy in the examined area of the 4$^{th}$ bearing of the engine block. The

overall average porosity is 1.69% for HD, and 0.74% for HDS. Samples cast without LSC have a 2.3 times higher porosity. There is also an apparent trend towards decreasing mechanical properties with increasing porosity. The relations sought for the resultant values of porosity measurements were, in particular, the relations $R_m$=f(P) and $R_{p0.2}$=f(P)[6]. The relations for the longitudinal section of HDS are in Fig. 8.

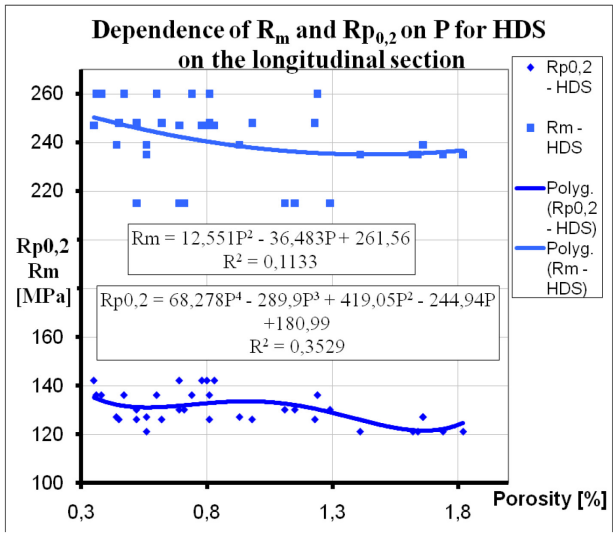


Fig. 8. Dependence of proof stress and ultimate strength on porosity for all measurements of longitudinal sections of HDS

The relations for the longitudinal section of HD are in Fig. 9.

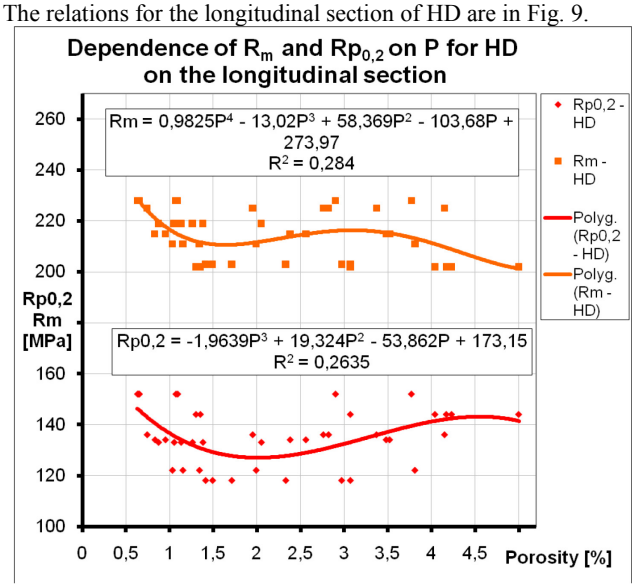


Fig. 9. Dependence of proof stress and ultimate strength on porosity for all measurements of longitudinal sections of HD

Average values for the longitudinal section in HDS (Fig. 10), values of all measurements of longitudinal sections in HD (Fig. 11).

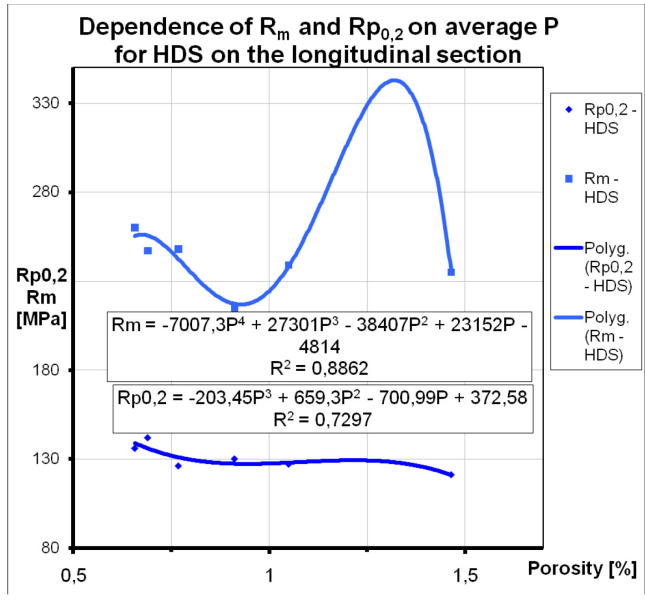


Fig. 10. Dependence of proof stress and ultimate strength on average porosity for all measurements of longitudinal sections of HDS

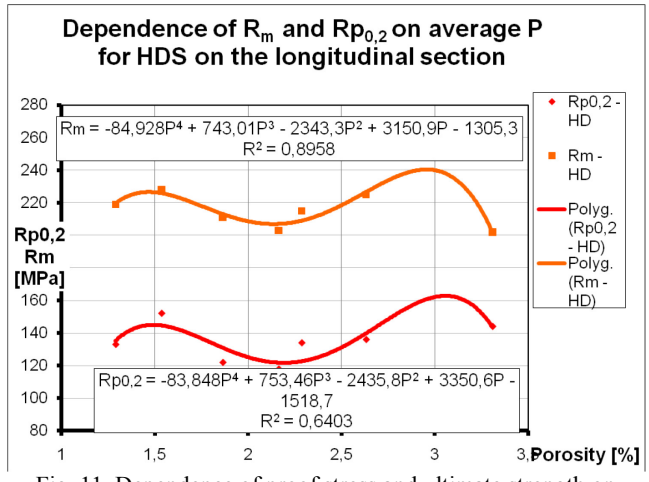


Fig. 11. Dependence of proof stress and ultimate strength on average porosity for all measurements of longitudinal sections of HD

## 2.3. Porosity simulation using the Magma software

The simulation of casting the AlSi9Cu3 aluminium alloy was preceded by networking the 3D CAD model. Porosity evaluation in the Magma program is based on the evaluation of percentage metal decrement in a given computation element. For this reason, a quantitative porosity comparison between the simulation program and the experiment is not quite correct since in the experiment the porosity percentage at the section site is evaluated, i.e. relative to the area being evaluated [11].

An absolute comparison of experimentally measured porosity and the results predicted by the simulation program is not quite feasible because MAGMA gives the measure of porosity as a concentrated shrinkage in a small material volume, i.e. in a magnitude of tens per cent. In die casting, porosity occurs rather diffusely over a larger volume. Also, values from the image output would have to agree exactly with the site of experimental sampling. On the whole, however, the values measured agree with the percentage-expressed porosity of the upper part from the MAGMA simulation program. Examples of the porosity measured can be seen in Fig. 12 (without LSC) and Fig. 13 (with LSC).

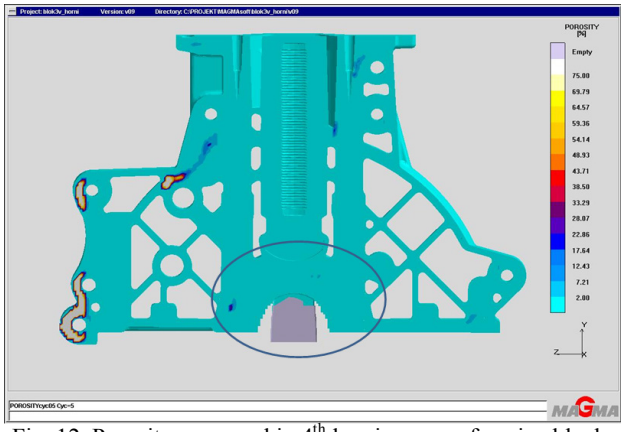

Fig. 12. Porosity measured in 4th-bearing area of engine block, die-cast without LSC, lateral view [6]

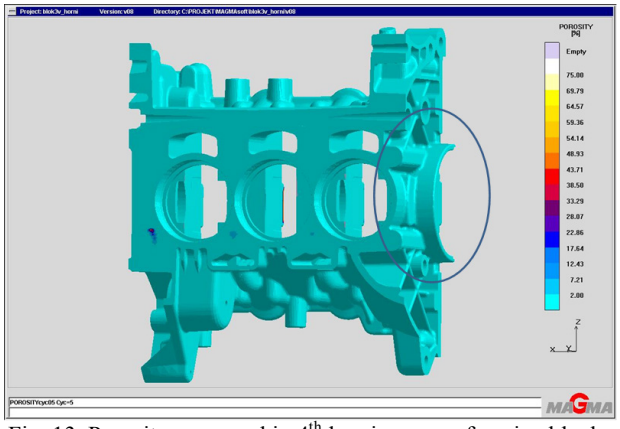

Fig. 13. Porosity measured in 4th-bearing area of engine block, die-cast with LSC, top view of bearing [6]

# 3. Conclusion

On the basis of a complex evaluation of experiments with HDS samples of the upper part of engine block cast with local squeeze casting and HD samples cast without local squeeze casting it can be said that the HD-series castings exhibit maximum porosity in the longitudinal section (average 2.15%; maximum 7.2%) and a total average porosity that is 2.3 times higher than in the HDS series. The HD series has a lower average ultimate strength. The graphs of porosity dependence exhibit considerable fluctuation in mechanical values, which may be due to inaccurate determination of $R_m$ and $R_{p0.2}$ and to the selection of the porosity site measured. The area of the upper engine block without LSC exhibits a certain decrease in mechanical properties and increase in porosity up to 5%. This still satisfies the norms prescribed in SKODA AUTO a. s.

# Acknowledgement

The present work was prepared with support from the project OPUS CZ.1.07./2.4.00/12.0029

# References

[1] Bähr, R., Todte, M. & Stroppe, H. (2006). Prediction of the influence of microstructure, porosity and residual stresses on strength properties of aluminium castings. In World Foundry Congress, 2006.

[2] Stroppe, H. (2000). Einfluss der Porosität auf die mechanischen Eigenschaften von Gusslegierung. *Giessereiforschung*. 52, 58-60.

[3] Čech, J., Říhová, M. & Lefner, J. (2010). Evaluation of effect of technological and metallurgical factors on porosity of die-cast Al alloys. *Slévárenství*. LVIII (5-6), 159-165. (in Czech).

[4] Lefner, J. (2009). *Evaluation of mechanical and structural properties of new block*. Diploma thesis, VUT FSI, Brno. (in Czech).

[5] Říhová, M. (2008). *Evaluation of porosity in gravity-cast Al-alloy castings*. Diploma thesis. VUT FSI, Brno. (in Czech).

[6] Havlíková, J. (2011). *Using simulation for prediction of defects and evaluation of properties in Al-alloy die-castings*. Diploma thesis. VUT FSI, Brno. (in Czech)

[7] Jirků, J. (2007). *Evaluation of porosity in Al-alloy die-castings*. Diploma thesis. VUT FSI, Brno. (in Czech).

[8] Klocová, P. (2008). *Evaluation of porosity in Al-alloy die-castings*. Diploma thesis. VUT FSI, Brno. (in Czech).

[9] Talanda, I. (2010). *Study of main factors affecting quality in technological processes*. Bachelor thesis. VUT FSI, Brno. (in Czech).

[10] Čech, J., Šolc, P., Krutiš, V. & Pecal, B. (2010). Prediction of porosity and microstructure in Al-alloy die castings, via simulation and experiment. *Slévárenství*. LVIII (3-4), 83-94. (in Czech).

[11] Čech, J., Říhová, M. & Havlíčková, J. (2012). Possibilities of evaluating porosity in die-cast Al alloys. to be published in *Slévárenství*. (in Czech).